JACS
JOURNAL OF THE AMERICAN CHEMICAL SOCIETY

ARTICLE

pubs.acs.org/JACS

A Small Molecule That Binds to an ATPase Domain of Hsc70 Promotes Membrane Trafficking of Mutant Cystic Fibrosis Transmembrane Conductance Regulator

Hyungseoph J. Cho,[†] Heon Yung Gee,[‡] Kyung-Hwa Baek,[†] Sung-Kyun Ko,[†] Jong-Moon Park,[§] Hookeun Lee,[§] Nam-Doo Kim,[∥] Min Goo Lee,[*,‡] and Injae Shin[*,†]

[†]Center for Biofunctional Molecules, Department of Chemistry, Yonsei University, Seoul 120-749, Korea

[‡]Department of Pharmacology, Brain Korea 21 Project for Medical Sciences, Yonsei University College of Medicine, Seoul 120-752, Korea

[§]Lee Gil Ya Cancer and Diabetes Institute, Gachon University of Medicine and Science, Incheon 406-840, Korea

[∥]New Drug Development Center, Daegu-Gyeongbuk Medical Innovation Foundation, Daegu 706-010, Korea

Supporting Information

ABSTRACT: Cystic fibrosis transmembrane conductance regulator (CFTR) is a cell-surface anion channel that permeates chloride and bicarbonate ions. The most frequent mutation of CFTR that causes cystic fibrosis is the deletion of phenylalanine at position 508 (ΔF508), which leads to defects in protein folding and cellular trafficking to the plasma membrane. The lack of the cell-surface CFTR results in a reduction in the lifespan due to chronic lung infection with progressive deterioration of lung function. Hsc70 plays a crucial role in degradation of mutant CFTR by the ubiquitin−proteasome system. To date, various Hsc70 inhibitors and transcription regulators have been tested to determine whether they correct the defective activity of mutant CFTR. However, they exhibited limited or questionable effects on restoring the chloride channel activity in cystic fibrosis cells. Herein, we show that a small molecule apoptozole (Az) has high cellular potency to promote membrane trafficking of mutant CFTR and its chloride channel activity in cystic fibrosis cells. Results from affinity chromatography and ATPase activity assay indicate that Az inhibits the ATPase activity of Hsc70 by binding to its ATPase domain. In addition, a ligand-directed protein labeling and molecular modeling studies also suggest the binding of Az to an ATPase domain, in particular, an ATP-binding pocket. It is proposed that Az suppresses ubiquitination of ΔF508-CFTR maybe by blocking interaction of the mutant with Hsc70 and CHIP, and, as a consequence, it enhances membrane trafficking of the mutant.

INTRODUCTION

CFTR is a cell-surface glycoprotein with two *N*-linked glycans and is an anion channel that permeates chloride and bicarbonate ions at the apical surface of epithelial cells.[1,2] Like other *N*-glycosylated proteins, an immaturely glycosylated CFTR (known as band B, ∼145 kDa) is initially produced by the cotranslational process in the rough endoplasmic reticulum (ER) (Figure 1A).[3] The immature form of CFTR is then transported to the Golgi complex where the maturely *N*-glycosylated CFTR (known as band C, ∼170 kDa) is formed. Finally, the mature CFTR migrates to the plasma membrane to act as a chloride channel.

CFTR has two membrane-spanning domains (MSD1 and MSD2), a regulatory (R) domain, and two nucleotide-binding domains (NBD1 and NBD2), as well as two *N*-glycans (Figure 1B). Because CFTR has a complex multidomain structure, it is intensively censored by the ER quality control (ERQC) and readily becomes a substrate of ER-associated degradation (ERAD). It has been reported that approximately 60% of the newly synthesized wild-type CFTR (wt-CFTR) is retained by ERQC and rapidly degraded by the ubiquitin-proteasome pathway.[4,5] Only about one-third of the precursor nascent CFTR is maturely glycosylated at the Golgi and expressed at the plasma membrane.[6]

The CFTR channel is activated for Cl^- efflux by cyclic AMP-dependent phosphorylation of multiple regulatory R-domain sites and by binding of ATP molecules to its NBDs.[7,8] The function of CFTR is to maintain ionic homeostasis and normal airway surface hydration. Defective trafficking of mutant CFTR to the plasma membrane is the major cause of cystic fibrosis, which is the most prevalent lethal genetic disease in Caucasians (one in approximately 2500).[9,10] The clinical features of cystic fibrosis are airway obstruction caused by thick mucus and chronic lung infection associated with *Pseudomonas aeruginosa*, which leads to the loss of lung function. Although a number of loss-of-function mutations in CFTR have been identified, deletion of

Received: July 20, 2011
Published: November 10, 2011

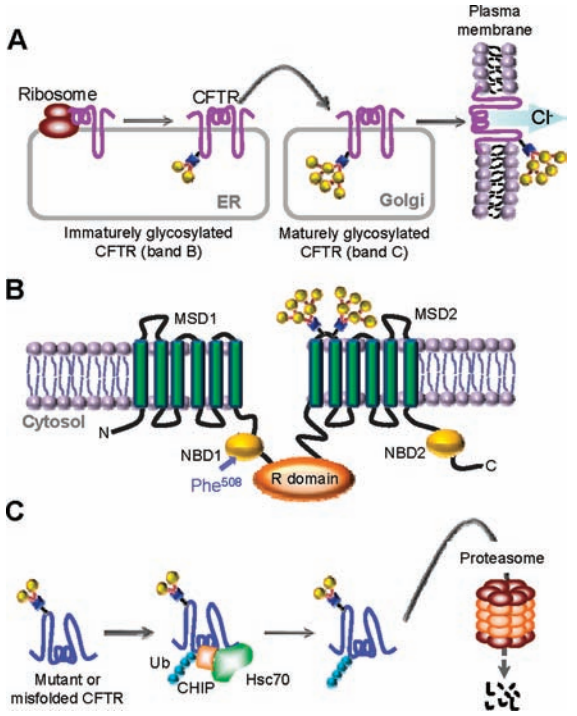

Figure 1. (A) Trafficking of folded wt-CFTR to the plasma membrane. Immaturely glycosylated CFTR (band B) in the ER moves to the Golgi where maturely glycosylated CFTR (band C) is formed. The mature form of CFTR is translocated to the plasma membrane to act as a chloride channel. (B) Representation of CFTR structure inserted into the plasma membrane (MSD, membrane-spanning domain; R domain, regulatory domain; NBD, nucleotide-binding domain; N, amino terminus; C, carboxy terminus). Two *N*-glycans are also indicated. (C) ER-associated degradation of mutant or misfolded CFTR. Mutant or misfolded CFTR is strongly recognized by Hsc70 followed by CHIP that has the ubiquitin (Ub) ligase activity. The ubiquitinated CFTR is removed by 20S proteasome.

phenylalanine at position 508 (ΔF508) located in the NBD1 of CFTR is found in ca. 70% of cystic fibrosis patients. Mutant ΔF508-CFTR has a temperature-sensitive folding defect.[4] At low temperature (~27 °C), some of mutant CFTR exit the ER to the plasma membrane, but it is prematurely degraded by a ubiquitin–proteosome system at higher temperature (37 °C). It has been suggested that nearly 99% of ΔF508-CFTR is degraded at 37 °C prior to its arrival at the cell surface, leading to impaired anion transport in epithelial cells.[5,11,12]

Proper folding of CFTR in the ER is highly dependent on a molecular chaperone heat shock cognate 70 (Hsc70). This chaperone protein is constitutively expressed in many cell types and has various functions such as protein folding, protein translocation, degradation of misfolded proteins, and regulation of assembly and disassembly of protein complexes. Hsc70 is composed of an N-terminal ATPase domain and a C-terminal substrate-binding domain (SBD) that have coupled activities.[13−15] The ATP-bound form of Hsc70 has a loose conformation of the SBD of Hsc70 and weak binding affinity for peptide/protein substrates. However, hydrolysis of ATP to ADP by the ATPase activity of Hsc70 induces conformational changes in the adjacent SBD, which lead to an increase in the binding affinity for substrates. Therefore, ATP hydrolysis is a major driving force behind the structural change and function of Hsc70.

Hsc70 interacts with wt- and ΔF508-CFTR with different binding affinities. It binds to mutant CFTR more tightly than wt-CFTR, and thus, in contrast to wt-CFTR, the mutant is incapable of dissociating from Hsc70.[16] As a result, mutant CFTR does not exit the ER to the Golgi where the mature glycosylated protein would be formed. When ΔF508-CFTR interacts with Hsc70, CHIP that recognizes the C-terminus of Hsc70 and has the ubiquitin ligase activity targets the mutant for proteasomal degradation by promoting its ubiquitination (Figure 1C).[17,18] Therefore, CHIP acts as a protein that converts Hsc70 from a protein-folding factor to a degradation factor in the ERQC. Importantly, ΔF508-CFTR rescued on the plasma membrane has a chloride channel function, although the rescued mutant is less stable than the wild-type protein,[19,20] and thus small molecules that block degradation of the mutant have potential applications as cystic fibrosis therapeutics.[21−24]

Despite having accumulated knowledge about its genetics, cystic fibrosis remains an incurable disorder. This serves a stimulus for research efforts aimed at the development of highly potent small molecules that can be employed to restore defective ΔF508-CFTR cellular processing. A growing body of evidence suggests that inhibition of Hsc70 activity can rescue defective cellular processing of mutant CFTR. Thus, inhibitors for Hsc70 are considered as potentially potent correctors that would promote membrane trafficking of mutant CFTR in the treatment of cystic fibrosis. To date, a number of Hsc70 inhibitors and its transcription regulators have been tested to determine if they enhance membrane trafficking of ΔF508-CFTR and restore the cell-surface chloride channel activity. For example, sodium 4-phenylbutyrate, which downregulates Hsc70 expression by enhancing its mRNA degradation, promotes ΔF508-CFTR maturation, but its reported effect on the CFTR chloride channel activity has been questioned.[25,26] Deoxyspergualin, which is an Hsc70 inhibitor that is used as an immunosuppressant, was found to partially restore cAMP-stimulated chloride channel activity in ΔF508-CFTR cells.[27] However, a mature form of ΔF508-CFTR was poorly transported to the plasma membrane in deoxyspergualin-treated cells. Recently, it was reported that an adamantyl sulfogalactosyl ceramide, which inhibits the Hsc70 activity by binding to its ATPase domain, suppressed ΔF508-CFTR degradation only during low-temperature glycerol rescue.[28] Thus, tested Hsc70 inhibitors or regulators have exhibited limited or questionable effects on restoring the chloride channel activity in cystic fibrosis cells. As a consequence, a great need still exists to develop Hsc70 inhibitors that have high potency to rescue a chloride-channel function in cystic fibrosis cells.

A small molecule apoptozole (Az, Figure 2A) that binds to cellular Hsc70 was recently identified from an imidazole library.[29] We designed a study to explore the utility of Az in rescuing defective ΔF508-CFTR cellular processing. Herein, we show that Az inhibits the ATPase activity of Hsc70 by binding to its ATPase domain and has high cellular potency to restore the chloride channel activity of mutant CFTR by promoting its membrane trafficking.

MATERIALS AND METHODS

Synthesis of 2. A solution of *p*-nitrophenyl chloroformate (72 mg, 0.36 mmol, 4 equiv) and 2,6-lutidine (104 μL, 0.9 mmol, 10 equiv) in anhydrous CH_2Cl_2 was added to a Wang resin (100 mg, 0.09 mmol, 1 equiv) in anhydrous CH_2Cl_2 (1 mL) at 0 °C.[30] After being shaken for 12 h at room temperature, the resin was washed with 10% DMF in CH_2Cl_2

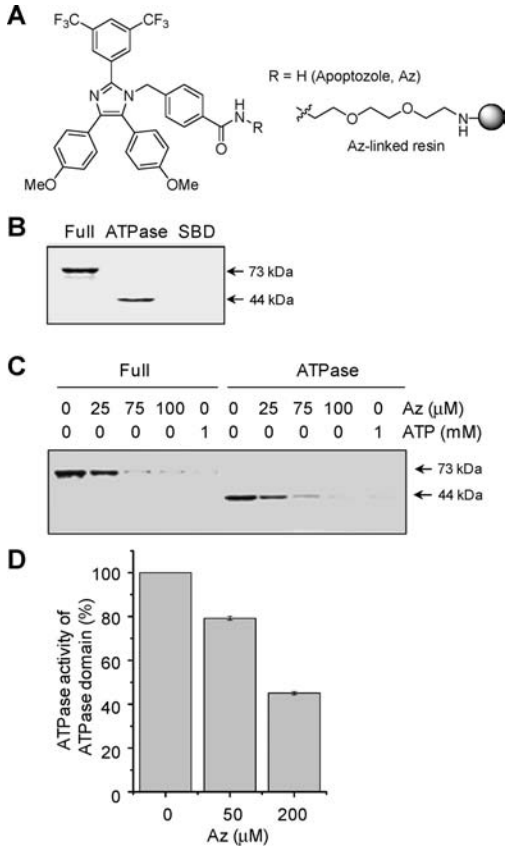

Figure 2. Az inhibits the ATPase activity of Hsc70 by binding to its ATPase domain. (A) Chemical structure of Az and an Az-linked resin. (B) The Az-linked resin was incubated with purified full-length or truncated His_6-tagged Hsc70 (ATPase domain and SBD). Proteins bound to the resin were visualized by silver staining. (C) The ATP-agarose was incubated with purified full-length or truncated Hsc70 in the absence or presence of Az or ATP. Proteins bound to the resin were visualized by silver staining. (D) Inhibition of the ATPase activity of an ATPase domain by Az. ATPase activities were measured by malachite green assay using 200 μM ATP (mean ± SD).

five times. A solution of 1,2-bis(2-aminoethoxy)ethane (40 μL, 0.27 mmol, 3 equiv) and DIEA (94 μL, 0.54 mmol, 6 equiv) in DMF was added to the resin. After being shaken for 6 h at room temperature, the resin was washed with 10% DMF in CH_2Cl_2 five times. A solution of DIEA (94 μL, 0.54 mmol, 6 equiv) and 3-(chlorosulfonyl)benzoyl chloride (69 μL, 0.45 mmol 5 equiv) in anhydrous CH_2Cl_2 was added to the resin at 0 °C. The mixture was stirred at 0 °C for 15 min and at room temperature for 3 h. The resin was washed with 10% DMF in CH_2Cl_2 five times. A solution of DIEA (94 μL, 0.54 mmol, 6 equiv), 4-dimethylaminopyridine (DMAP, 1.1 mg, 0.009 mmol, 0.1 equiv), and 7-(diethylamino)-*N*-(2-(2-hydroxyethoxy)ethyl)-2-oxo-2*H*-chromene-3-carboxamide (95 mg, 0.27 mmol, 3 equiv) in anhydrous CH_2Cl_2 was added to the resin, and the mixture was stirred at room temperature for 12 h. The assembled compound was cleaved from a solid support by treatment with trifluoroacetic acid (TFA)-triethylsilane (TES) (98:2) for 1 h. After removal of solvent, the crude residue was purified by preparative reversed-phase HPLC to give **2**: ^{1}H NMR ($CDCl_3$, 400 MHz) δ 9.09 (t, J = 4.0 Hz, 1H), 8.67 (s, 1H), 8.44 (s, 1H), 8.28 (br s, 1H), 8.24 (d, J = 7.6 Hz, 1H), 8.05 (br s, 2H), 8.00 (d, J = 8.0 Hz, 1H), 7.61 (t, J = 8.0 Hz, 1H), 7.47 (d, J = 8.8 Hz, 1H), 6.68 (dd, J = 9.4, 2.4 Hz, 1H), 6.51 (d, J = 2.4 Hz, 1H), 5.43 (br s, 1H), 4.22 (t, J = 4.0 Hz, 2H), 3.82 (t, J = 4.4 Hz, 2H), 3.70−3.67 (m, 11H), 3.58−3.46 (m, 9H), 3.32 (br s, H), 1.26 (t, J = 7.2 Hz, 6 H); ^{13}C NMR (100 MHz, CD_3OD) δ 168.1, 165.4, 164.0, 159.2, 154.7, 149.4, 138.1, 137.0, 133.7, 132.7, 131.9, 131.0, 127.8, 111.7, 110.1, 109.5, 97.3, 71.5, 71.4, 71.3, 70.5, 70.5, 69.5, 67.9, 54.8, 46.0, 40.9, 40.7, 40.3, 12.7; MALDI-TOF-MS calcd for $C_{31}H_{43}N_4O_{10}S$ $[M + 1]^+$ 663.2622, found 663.2451.

Synthesis of 3. The stirred solution of 3,5-bis(trifluoromethyl)-benzaldehyde (283 μL, 1.72 mmol, 1.3 equiv), 4,4′-dimethoxybenzil (464 mg, 1.72 mmol, 1.3 equiv), 4-(aminomethyl)benzoic acid (200 mg, 4 mmol, 1 equiv), and ammonium acetate (612 mg, 7.94 mmol, 6 equiv) in acetic acid (6 mL) was heated for 12 h at 100 °C. The reaction mixture was cooled to room temperature, diluted with ethyl acetate, and washed with water, saturated $NaHCO_3$, and brine. The organic layer was dried over $MgSO_4$, filtered, and concentrated under the reduced pressure. The crude product was purified by flash column chromatography (CH_2Cl_2/MeOH 10:1) to give **3** in 48% yield: ^{1}H NMR ($CDCl_3$, 400 MHz) δ 8.07 (s, 2H), 8.00 (d, J = 8.4 Hz, 2H), 7.83 (s, Hz, 1H), 7.52 (dd, J = 6.8, 2.4 Hz, 2H), 7.18 (dd, J = 6.8, 2.0 Hz, 2H), 6.99 (d, J = 8.4, 2H), 6.89 (dd, J = 6.9, 2.0 Hz, 2H), 6.80 (dd, J = 6.8, 2.0 Hz, 2H), 5.16 (s, 2H), 3.82 (s, 3H), 3.77 (s, 3H); ^{13}C NMR (DMSO, 100 MHz) δ 167.0, 159.7, 158.1, 143.3, 141.8, 137.6, 133.0, 132.2, 130.8, 130.6, 130.4, 129.7, 128.4, 127.4, 126.7, 125.8, 124.4, 121.8, 121.7, 114.7, 113.7, 55.1, 55.0, 47.7; MALDI-TOF-MS calcd for $C_{33}H_{25}F_6N_2O_4$ $[M + 1]^+$ 627.1713, found 627.1136.

Synthesis of Az-Conjugated Probe 1. To a solution of **2** (3 mg, 4.5 μmol, 1 equiv) in anhydrous DMF (5 mL) were added **3** (2 mg, 10.0 μmol, 2.2 equiv), DIEA (3.9 μL, 22.6 μmol, 5 equiv), and 1-ethyl-3-(3-dimethylaminopropyl)-carbodiimide (EDC) (1.7 mg, 9.1 μmol, 2 equiv). The mixture was stirred at room temperature for 6 h. The reaction mixture was diluted with ethyl acetate, and washed with water, saturated $NaHCO_3$, and brine. The organic layer was dried over anhydrous Na_2SO_4, filtered, and concentrated under the reduced pressure. The crude residue was purified by preparative reversed-phase HPLC to give **1**: ^{1}H NMR (400 MHz; $CDCl_3$) δ 8.92 (br s, 1H), 8.66 (s, 1H), 8.38 (s, 1H), 8.16 (d, J = 7.6 Hz, 1H), 8.06 (s, 2H), 8.03 (d, J = 8.0 Hz, 1H), 7.81 (s, 1H), 7.74 (d, J = 8.4 Hz, 2H), 7.60 (t, J = 5.2 Hz, 1H), 7.50 (d, J = 8.8 Hz, 2H), 7.40 (d, J = 9.2 Hz, 1H), 7.18 (d, J = 8.4 Hz, 2H), 6.96 (d, J = 8.0 Hz, 2H), 6.89 (d, J = 8.8 Hz, 2H), 6.80 (d, J = 8.8 Hz, 2H), 6.64 (dd, J = 9.2, 2.4 Hz, 1H), 6.48 (dd, J = 8.4, 2.4 Hz, 1H), 5.13 (s, 2H), 4.88 (br s, 2H), 4.21 (t, J = 4.4 Hz, 2H), 3.83 (s, 3H), 3.82 (s, 3H), 3.702 (s, 1H), 3.66−3.60 (m, 12H), 3.52−3.42 (m, 9H), 1.23 (t, J = 7.2 Hz, 6H); MALDI-TOF-MS calcd for $C_{64}H_{65}F_6N_6O_{13}S$ $[M + 1]^+$ 1271.4156, found 1271.3466.

Synthesis of Cy3-Az. To a stirred solution of *N*-2-(2-(2-aminoethoxy)ethoxy)ethylated apoptozole[29,31,32] (27 mg, 36 μmol, 1 equiv) in DMF were added *N*-hydroxybenzotriazole (HOBT, 8 mg, 39.6 μmol, 1 equiv), 2-(1*H*-benzotriazole-1-yl)-1,1,3,3-tetramethyl-uronium hexafluorophosphate (HBTU, 15 mg, 39.6 μmol, 1.1 equiv), diisopropylethylamine (DIEA, 13 μL, 72 μmol, 2 equiv), and carboxylic acid-containing Cy3 (16 mg, 36 μmol, 1 equiv). After being stirred for 8 h at room temperature, the reaction mixture was diluted with ethyl acetate. The organic layer was washed with brine, dried over anhydrous Na_2SO_4, filtered, and concentrated under reduced pressure. The crude product was purified by flash column chromatography (CH_2Cl_2/MeOH 10:1) to give Cy3-Az in 24% yield: ^{1}H NMR (400 MHz, $CDCl_3$) δ 8.38 (t, 1H, J = 13.2 Hz), 8.07 (s, 2H), 8.02 (d, 2H, J = 8.0 Hz), 7.78 (s, 1H), 7.49 (d, 2H, J = 8.5 Hz), 7.40−7.33 (m, 4H), 7.26−7.20 (m, 4H), 7.17 (d, 2H, J = 8.7 Hz), 7.11 (d, 1H, J = 7.9 Hz), 7.03 (d, 1H, J = 5.5 Hz), 6.99 (d, 2H, J = 8.2 Hz), 6.87 (d, 2H, J = 8.0 Hz), 6.77 (d, 2H, J = 8.8 Hz), 5.11 (s, 2H), 4.13 (t, 2H, J = 7.5 Hz), 3.80 (s, 3H), 3.76 (s, 3H), 3.70−3.61 (m, 13H), 3.47 (dd, 2H, J = 5.1, 10.7 Hz), 2.54 (t, 2H, J = 6.8 Hz), 1.87 (t, 2H, J = 7.4 Hz), 1.69 (m, 14H); ^{13}C NMR (400 MHz $CDCl_3$): 174.7, 174.0, 173.4, 166.9, 160.2, 158.6, 150.8, 144.3, 142.7, 141.9, 140.6, 140.5, 140.2, 139.0, 134.2, 133.0, 132.4, 132.2, 131.9, 130.7, 129.2, 129.1, 128.7, 128.2, 128.1, 126.8, 125.9, 125.8, 125.6, 122.2, 122.1, 121.8, 114.8, 113.8, 111.1, 110.9, 104.0, 103.5, 70.3, 69.8, 55.4, 55.3, 49.2, 49.1, 48.3, 44.4,

39.9, 39.3, 36.1, 31.4, 28.2, 28.2, 27.0, 23.2; MALDI-TOF-MS calcd for $C_{68}H_{71}F_6N_6O_6^+$ $[M + H]^+$ 1182.533, found 1182.0668.

Binding of Az to an ATPase Domain of Hsc70. The Az-linked resin or ATP-agarose (Sigma, A-9264) was incubated with 2−5 μg of purified proteins (full-length and truncated Hsc70 (ATPase domain or SBD)) and identical volume of bead buffer [10 mM Tris (pH 7.4), 5 mM NaF, 250 mM NaCl, 5 mM EDTA, 5 mM EGTA, 0.1% Triton X-100 and protease inhibitor cocktail (Roche) per 20 mL of buffer] at 4 °C for 1 h. For competition experiments, various concentrations of Az or 1 mM ATP were added to the protein extract in bead buffer, and the mixture was incubated at 4 °C for 30 min. The Az-linked resin or ATP-agarose was incubated with protein extract pretreated with the competitor. The supernatant containing unbound proteins was removed by centrifugation at 2000 rpm for 1 min, and the matrices were washed seven times with 1 mL of bead buffer. Proteins bound to the matrices were detached by treating with 30 μL of Laemmli buffer (Bio-Rad) at 94 °C for 5 min. The detached proteins were separated by 10% SDS-PAGE and visualized by silver staining.

Measurements of ATPase Activities of Hsc70. The assay was performed under the previous publication with modifications.[33] Stock solutions of malachite green (0.081% w/v), polyvinyl alcohol (2.3% w/v), and ammonium heptamolybdate tetrahydrate (5.7% w/v in 6 M HCl) were prepared and stored at 4 °C. Three solutions were mixed with water in the ratio of 2:1:1:2 to prepare the malachite green reagent. For determination of the ATPase activity, a master mixture of purified ATPase domain was prepared in assay buffer (100 mM Tris-HCl, 20 mM KCl, and 6 mM $MgCl_2$, pH 7.4) as final concentration of 2 μM. An aliquot (10 μL) of this mixture was added into each well of a 96-well plate. To this solution was added 9 μL of Az in assay buffer, and the plate was incubated for 30 min at room temperature. To start the reaction, 1 μL of 4 mM ATP was added to the solution. The final concentrations were 1 μM protein, 50 or 200 μM Az, and 200 μM ATP in 20 μL of assay buffer. After 3 h incubation at 37 °C, 80 μL of malachite green reagent was added into each well. The samples were mixed thoroughly and incubated at 37 °C for 15 min, and 10 μL of 34% sodium citrate was added to stop the nonenzymatic hydrolysis of ATP. The absorbance was determined at 620 nm on a SpectraMax 340 PC 384 (Molecular Devices, Sunnyvale, CA). To correct nonenzymatic hydrolysis of ATP, the absorbance from ATP in identically treated buffer lacking proteins was subtracted.

Identification of Amino Acid Labeled by a Fragment of 1 by MS Analysis. Purified Hsc70 was incubated with Az-conjugated probe **1** (2 equiv) in reaction buffer (6 mM $MgCl_2$, 60 mM KCl and 100 mM Tris-HCl, pH 7.4) for 2 days at 37 °C. The protein was treated with 6 M urea for denaturation and then 5 mM tris(2-carboxyethyl)phosphine for reduction at 37 °C for 0.5 h. Samples were adjusted to pH 8 with 1 M Tris-HCl (pH 8.3) and then incubated with 15 mM iodoacetamide at room temperature for 1 h in the dark to block cysteine residues. The urea concentration of the solution was adjusted to below 2 M with 10 mM Tris buffer. The protein was then digested with sequencing grade modified trypsin (Promega) in trypsin resuspension buffer (Promega) for 16 h at 37 °C. The samples were subjected to C18 spin column (Harvard Apparatus) and SCX column chromatography (OPTIMIZE Technologies) to remove interfering substances. The digested peptide samples were dried using Speedvac (SCANVAC, Bio-Rad) and resuspended with 100 μL of water containing 0.1% formic acid for MS analysis. The peptides were separated by a 1200 series HPLC system (Agilent Technologies) using HPLC-chip (large capacity chip, 150 mm, 300 Å, C18 chip, w/160 nL trap column, Agilent Technologies) with a nanoflow pump. MS analysis was performed using a 6520 Accurate-Mass Q-TOF LC/MS (Agilent Technologies) with a HPLC-chip cube source. Data were acquired in the mass range from 100 to 3000 m/z with positive ion polarity and 3.7 V collision energy. Acquisition rate was set per a second of three spectra. The peak list resulting from MS/MS was exported to mzXML format, and the generated peak lists (.mzXML) were searched by SEQUEST against the International Protein Index (IPI) human database (v3.75) from the European Bioinformatics Institute. Search results were evaluated with the trans-proteomic pipeline (TPP) using Peptide Prophet (v4.4.1). The peptide peak with increased mass (330.1580 Da) of a fragment of **1** was identified.

Molecular Modeling. The crystal structure of Hsc70 from Protein Data Bank (PDB code 3FZM, an ATP-bound form) was used for docking simulation. PDB files were processed by removing all solvents, counterions, and substrates. For the docking, the structure of Hsc70 was kept rigid, whereas all of the torsional bonds in Az were set free to flexible docking. Affinity grids on the binding pocket were constructed using AutoGrid4 with grid spacing of 0.375 Å. Each grid map consisted of 50 × 50 × 50 grid points. Autodock4 was used to find the binding positions for Az on the Hsc70 by docking simulation. Docking was performed by a global genetic algorithm combined with local minimization and Lamarckian genetic algorithm to explore the compound conformational space. Each docking job with 100 trials was performed, and final docked conformations were clustered using a tolerance of 1 Å root-mean-square deviation. All other parameters were set to default values. The docking conformation properly oriented toward the ATPase binding pocket was selected, and the free energy of binding was estimated. The molecular graphics for the inhibitor binding pocket and refined docking model for the selected Az was generated using PyMol package (http://www.pymol.org).

Biochemical Studies and Cell Experiments. For details of biochemical studies and cell experiments, see the Supporting Information.

RESULTS AND DISCUSSION

Az Inhibits Hsc70 Activity by Binding to Its ATPase Domain. We previously showed that Az bound to Hsc70 (a constitutive form) and Hsp70 (an inducible form).[29] However, the binding site of Az toward these proteins was not investigated at that time. Because Hsc70 is a more attractive target for cystic fibrosis treatment, its inhibitors have been tested for restoration of mutant CFTR on the plasma membrane in cystic fibrosis cells.[25−28] Therefore, in this study, we have focused on Hsc70 to elucidate the molecular mechanism of restoration of mutant CFTR on the plasma membrane induced by Az.

We initially determined if Az binds to an ATPase domain or an SBD of Hsc70. For this purpose, affinity chromatography was carried out using purified proteins and an Az-linked resin. Full-length and truncated (ATPase domain, 1−386 residues; and SBD, 387−646 residues) Hsc70 proteins were isolated in their N-terminal His_6-tagged forms (Figure S1). As shown in Figure 2B, while the full-length protein and an ATPase domain bind to the Az-linked resin, an SBD does not. To further investigate whether Az interacts with an ATPase domain, competition experiments were performed to elucidate binding of Hsc70 to ATP-agarose in the presence and absence of Az. The results show that the full-length protein and the ATPase domain both bind to the ATP-resin in the absence of Az and ATP, but they rarely interact with this resin in the presence of 75−100 μM Az or 1 mM ATP (Figure 2C). The ability of Az to inhibit the ATPase activity of Hsc70 was evaluated next. It was found that Az suppressed the ATPase activity of an ATPase domain by 20% at 50 μM and 55% at 200 μM based on the malachite green assay using 200 μM ATP (Figure 2D). The results combined with those arising from affinity chromatography investigations suggest that Az inhibits the Hsc70 activity by binding to its ATPase domain.

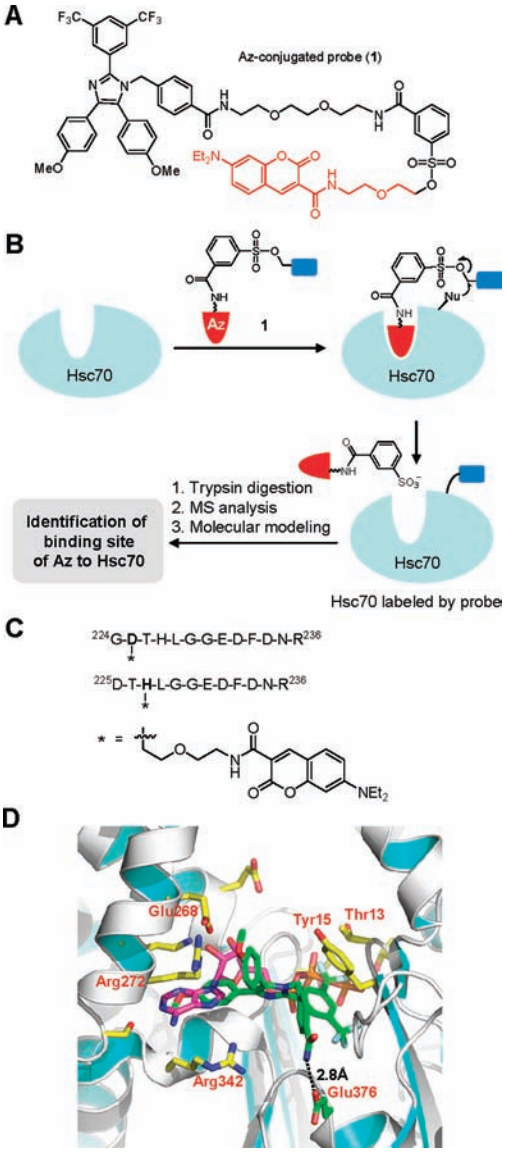

Figure 3. (A) Chemical structure of Az-conjugated probe **1**. (B) Schematic illustration of the strategy used to identify the binding site of Hsc70 for Az using **1**. Binding of **1** to Hsc70 promotes protein labeling via an S_N2-type reaction. The binding site of Hsc70 for Az can be identified by mass spectrometry after trypsin digestion (Nu: a nucleophilic amino acid residue). (C) Sequence of the labeled peptides identified by nanoLC-MS/MS analysis. His227 (major) and Asp225 (minor) were labeled by a fragment of **1**. (D) Docking model of Az (green)/Hsc70 (PDB code 3FZM) superimposed with ATP (red, adenosine; orange, triphosphate).

To investigate the detailed binding mode of Az to Hsc70, a ligand-directed protein labeling method, developed by the Hamachi group,[34] with Az-conjugated probe **1** was employed. In the probe, Az is connected with diethylaminocoumarin via a sulfonate as a reactive group (Figure 3A). Binding of an Az moiety in **1** to Hsc70 promotes a reaction of the reactive group with a nucleophilic amino acid residue located near the binding site of the protein (Figure 3B). When this chemical event occurs, Hsc70 is modified by a part of **1** because an Az-containing moiety is released from the probe via an S_N2-type reaction. The labeled amino acid is then identified by using mass spectrometric peptide mapping analysis.

Scheme 1. Synthesis of Az-Conjugated Probe 1

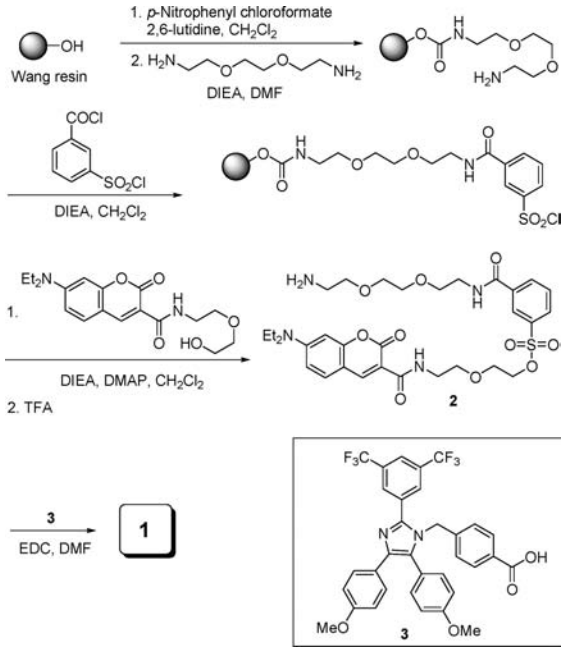

The required probe **1** was prepared as delineated in Scheme 1. To facilitate its synthesis, we employed the combined solid-phase with solution-phase chemistry. Compound **2** was obtained after release of the product assembled on a solid support and then reacted with carboxylic acid-containing **3** in the presence of coupling reagents to give the probe **1**.

To identify the binding site of Az to Hsc70, purified full-length Hsc70 was incubated with **1** (2 equiv) for 48 h at 37 °C. After treatment of the mixture with trypsin, the digested peptides were analyzed by using nano-LC-MS/MS. The peptide peak with increased mass (330 Da) of a fragment (red part in Figure 3A) of **1** was identified by MS/MS. The results of peptide mapping analysis reveal that His227 (major) and Asp225 (minor) are modified by a fragment of **1** (Figure 3C and Figure S2). Because both residues are located at the entrance of the ATP-binding pocket, the protein labeling study suggests that Az recognizes an ATPase domain, maybe an ATP-binding pocket of Hsc70.

To obtain more information on the binding mode of Az to Hsc70, molecular docking studies with Hsc70 (PDB code 3FZM, a ATP-bound form) were performed.[35] An analysis of the docking model suggests that Az can adopt a conformation that overlays with ATP (Figure 3D and Figure S3). In this model, the 3,5-bis(trifluoromethyl)phenyl group of Az interacts with the binding site of a triphosphate moiety of ATP through polar interactions,[36] and the two 4-methoxy phenyl moieties of Az are located at the adenosine binding site of Hsc70. Also, the analysis suggests that the $CONH_2$ group of Az can interact with the Glu376 side chain of Hsc70 via a hydrogen-bonding interaction. Molecular modeling studies of the complex between **1** and Hsc70 was performed to analyze the results obtained from the ligand-directed protein labeling study. Using theoretical techniques, a plausible binding model of **1** with Hsc70 was presented (Figure S4), in which the tosyl group of **1** is located near the imidazole side chain of His227 (~4 Å from the tosyl group) at the entrance of the ATP-binding site. This location nicely explains the mainly observed labeling of the His227 residue by **1** via an S_N2-type

dx.doi.org/10.1021/ja206762p |J. Am. Chem. Soc. 2011, 133, 20267–20276

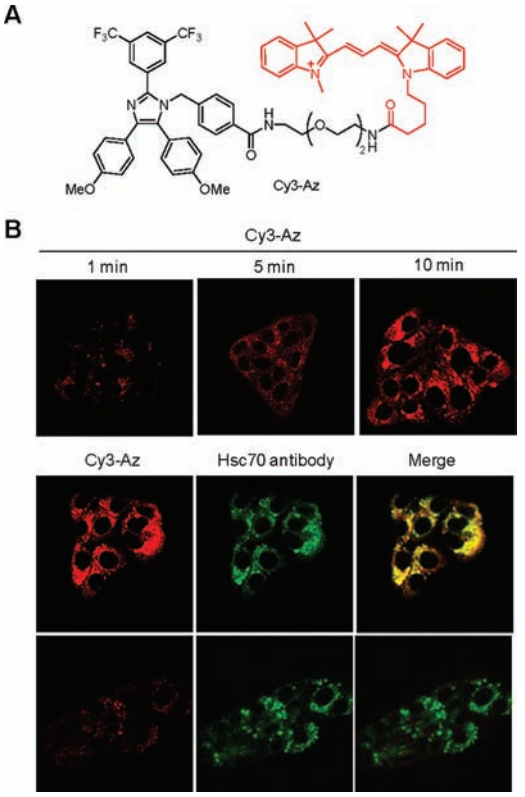

Figure 4. (A) Chemical structure of Cy3-Az. (B) Fluorescent images of Capan-1 cells treated with 200 nM Cy3-Az for 1, 5, and 10 min (upper), treated with 200 nM Cy3-Az and then anti-Hsc70 antibody (middle), and pretreated with 5 μM Az for 1 h followed by sequential treatment with 200 nM Cy3-Az and Hsc70 antibody (lower).

reaction. The molecular modeling studies together with the biochemical results strongly suggest that Az inhibits Hsc70 activity by binding to its ATPase domain, presumably the ATP-binding pocket.

To examine whether Az interacts with cellular Hsc70, Capan-1 cells originating from pancreatic epithelial cells expressing wt-CFTR were treated with Cy3-conjugated Az (Cy3-Az, Figure 4A) for 0.5 h and then incubated with anti-Hsc70 antibody. The results of fluorescence microscopy analysis show that fluorescence of Cy3-Az is largely overlapped with Hsc70 in the cytoplasm (Figure 4B, middle). The extensive wash of the treated cells has little influence on the fluorescence intensity of Cy3-Az. In contrast, pretreatment of cells with excess Az (5 μM) for 1 h remarkably reduces the fluorescence intensity of Cy3-Az (Figure 4B, lower). These and biochemical results indicate that Az interacts with cellular Hsc70.

Az Treatment Enhances ΔF508-CFTR Trafficking to the Plasma Membrane. Because Az has its inhibitory activity toward Hsc70, we tested whether this inhibitor could restore defective trafficking of ΔF508-CFTR to the plasma membrane as suggested previously. Initially, cell-surface expression of mutant CFTR was examined by using immunocytochemical analysis with anti-CFTR antibody. CFPAC-1 cells (cells expressing ΔF508-CFTR), originating from pancreatic duct cells of a patient with cystic fibrosis, were exposed for 24 h at 37 °C to 200 nM Az, a concentration at which cell death is not observed by MTT assay (Figure S5). Capan-1 cells (cells expressing wt-CFTR) were incubated as a control for 24 h at 37 °C without treatment with Az. An ER tracker was used to visualize the ER. As expected, a large fraction of

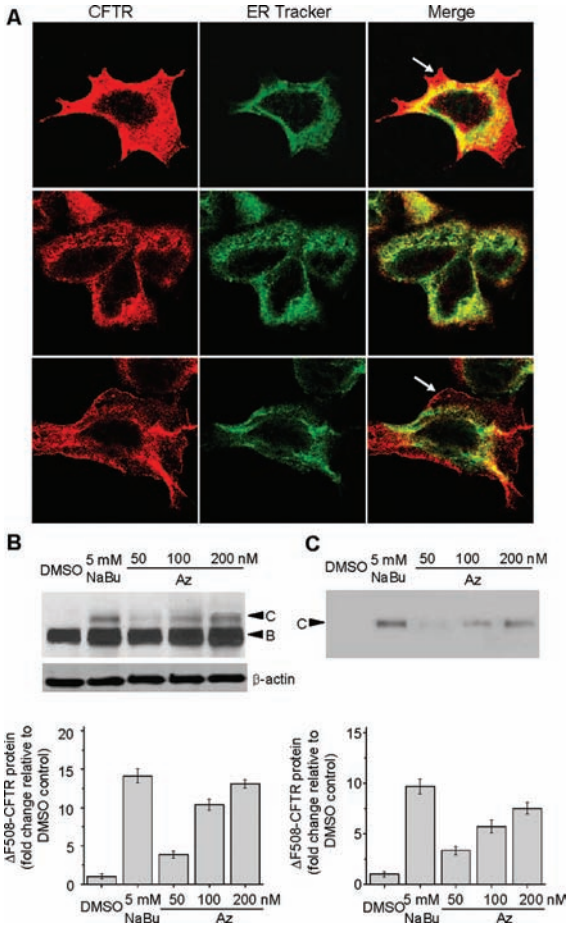

Figure 5. Az treatment enhances membrane trafficking of ΔF508-CFTR. (A) Wt-CFTR HEK cells untreated with Az (upper), ΔF508-CFTR HEK cells untreated with Az (middle), and treated with 200 nM Az for 24 h at 37 °C (lower). All cells were stained with anti-CFTR antibody and ER tracker. Arrows indicate cell-surface wt- and mutant CFTR. (B) Expression of ΔF508-CFTR after 24 h treatment of ΔF508-CFTR HEK cells with various concentrations of Az at 37 °C. (C) Detection of cell-surface ΔF508-CFTR after 24 h treatment of ΔF508-CFTR HEK cells with 200 nM Az at 37 °C followed by biotinylation of the cell-surface proteins with EZ-Link sulfo-NHS-SS-biotin (B and C: mean ± SD).

wt-CFTR is produced on the plasma membrane in Capan-1 cells, but ΔF508-CFTR is rarely expressed at the plasma membrane in untreated CFPAC-1 cells where it is spread mostly over the cytoplasma, in particular, the ER (Figure S6, upper and middle panels). Importantly, a significant amount of the endogenous mutant protein is expressed at the surface of CFPAC-1 cells treated with Az (Figure S6, lower panels). To probe this further, HEK293 cells (human embryonic kidney cells) were stably transfected with wt- and ΔF508-CFTR (wt-CFTR HEK and ΔF508-CFTR HEK cells, respectively) and then incubated with or without 200 nM Az for 24 h at 37 °C. The immunocytochemical analysis shows that ΔF508-CFTR is rarely expressed at the plasma membrane in the absence of Az; however, a significant amount of the mutant is expressed at the cell surface in the presence of Az (Figure 5A, middle and lower panels). These results suggest the potential role of Az in rescuing the mutant CFTR trafficking defect.

Trafficking of CFTR from the ER to the plasma membrane can be also monitored by observing a change in its migration on

SDS- PAGE. The immaturely glycosylated, ER-localized CFTR (band B) is processed in the Golgi to produce the maturely glycosylated, plasma membrane-localized CFTR (band C) that migrates more slowly than band B on PAGE. In this analysis, ΔF508-CFTR HEK cells were incubated with Az or the non-specific transcriptional regulator sodium butyrate (NaBu), which serves as a positive control that partially rescues folding defects of mutant CFTR and induces its band C formation.[37] We observed an increase in the level of band C of mutant CFTR after 24 h treatment of ΔF508-CFTR HEK cells with 200 nM Az. This level is similar to that of mutant CFTR obtained after 24 h treatment with 5 mM NaBu (Figure 5B). Furthermore, the plasma membrane-localization of ΔF508-CFTR was determined after cell-surface biotinylation. ΔF508-CFTR HEK cells were initially treated with 200 nM Az for 24 h and then exposed to cell-impermeable EZ-Link sulfo-NHS-SS-biotin (Pierce) to label the cell-surface proteins. The biotinylated surface proteins were isolated by using streptavidin-conjugated beads. As shown in Figure 5C, the maturely glycosylated CFTR (band C) was formed in a dose-dependent manner in Az-treated cells, which is consistent with results obtained from whole cell analysis.

To address whether Az affects transcriptional levels like other transcriptional regulators, mRNA levels of CFTR and ΔF508-CFTR were analyzed by using RT-PCR. Their mRNA levels are not changed in both wt- and ΔF508-CFTR HEK cells treated with Az (Figure S7). These results suggest that Az treatment induces the enhanced expression of cell-surface ΔF508-CFTR without affecting its transcriptional levels.

It has been reported that rescued ΔF508-CFTR has a temperature-sensitive stability in post-ER compartments, including the cell surface.[20] To assess whether Az also affects the stability of rescued, cell-surface ΔF508-CFTR, we measured the half-life of rescued mutant CFTR after blocking protein biosynthesis with cycloheximide. Wt-CFTR HEK cells were treated with cycloheximide at 37 °C to prevent the new production of CFTR. In addition, ΔF508-CFTR HEK cells were incubated for 24 h at 27 °C to promote trafficking of the mutant to the plasma membrane because the reduced temperature partially corrects the mutant CFTR trafficking defect. After accumulation of mutant CFTR, the cells were exposed to 50 μg/mL of cycloheximide at 37 °C. On the other hand, ΔF508-CFTR HEK cells were treated with 200 nM Az at 37 °C for 24 h and subsequently with 50 μg/mL of cycloheximide. The level of the mature form (band C) of CFTR in cells was determined by using quantitative immunoblotting as a function of incubation time. The densitometric analysis reveals that the half-life of the rescued ΔF508-CFTR ($t_{1/2} \approx 5$ h) after incubation at 27 °C is approximately 4 times shorter than that of the wt-CFTR ($t_{1/2} \approx 19$ h) at 37 °C (Figure 6), a finding that is consistent with previous results.[20] Interestingly, treatment of cells with 200 nM Az at 37 °C for 24 h leads to increased stability of rescued mutant CFTR ($t_{1/2} \approx$ 7.5 h) in comparison with that of mutant CFTR rescued by incubation at 27 °C. Our data suggest that Az not only enhances trafficking of the mutant protein to the plasma membrane, but also it promotes increased stability of the rescued, cell-surface mutant CFTR.

Membrane proteins with non-native conformations, which have escaped from the ER or are generated in post-ER compartments, are continuously censored by peripheral quality control and preferentially eliminated through lysosomal degradation. Recently, it has been suggested that Hsc70 also plays an important role in peripheral quality control of ΔF508-CFTR.[38]

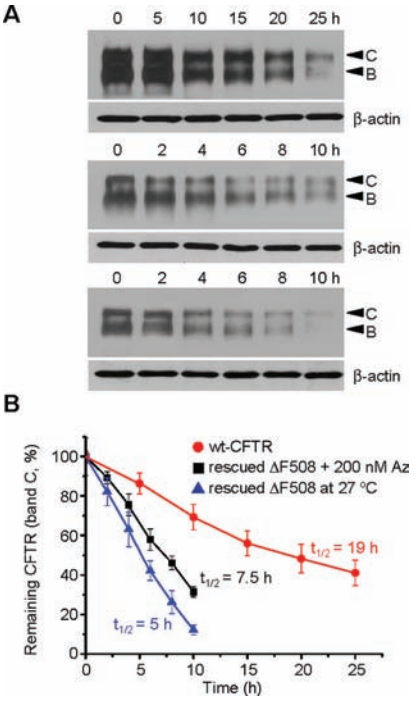

Figure 6. Effect of Az on the stability of cell-surface CFTR. (A) Upper: Wt-CFTR HEK cells were treated with 50 μg/mL of cycloheximide at 37 °C, and then CFTR was immunoblotted using CFTR antibody after the indicated time. Middle: ΔF508-CFTR HEK cells were treated with 200 nM Az for 24 h at 37 °C and then treated with 50 μg/mL of cycloheximide. Mutant CFTR was immunoblotted using CFTR antibody. Lower: ΔF508-CFTR HEK cells were incubated with 50 μg/mL of cycloheximide at 27 °C and then mutant CFTR was immunoblotted. (B) Half-life determination of the cell-surface wt- and ΔF508-CFTR (band C). Band C was calculated from the densitometric analysis of immunoblots shown in (A) (mean ± SD).

Therefore, in addition to the escape from ERQC, inhibition of Hsc70 by Az may provide the additional benefit of increased cell surface stability of mutant CFTR through an effect on peripheral quality control.

Rescue of the Chloride Channel Activity of ΔF508-CFTR by Az. The plasma membrane localization of a maturely glycosylated form of ΔF508-CFTR by Az suggests that Az treatment may induce recovery of the chloride channel activity. To examine the effect of Az on the cAMP-activated chloride channel activity of ΔF508-CFTR, Cl^- permeability in CFPAC-1 cells was monitored by examining the Cl^-/NO_3^- exchange activity using microfluorometric measurement of $[Cl^-]$. Intracellular chloride ions were detected using the Cl^--quenching fluorescent indicator *N*-(ethoxycarbonylmethyl)-6-methoxyquinolinium bromide (MQAE).[39] Changes in the fluorescence intensity of the cytosolic dye were observed by applying 145 mM NO_3^- solution to MQAE-pretreated CFPAC-1 cells in 145 mM Cl^- with cAMP stimulation using 100 μM IBMX (3-isobutyl-1-methylxanthine) and 5 μM forskolin. In the absence of Az, little fluorescence change of MQAE is observed in CFPAC-1 cells (Figure 7A, black line). In contrast, cells exposed to 200 nM Az for 24 h exhibit a remarkable increase in MQAE fluorescence (Figure 7A, red line), indicating that a reduction of the intracellular Cl^- concentration takes place through Cl^- efflux. Furthermore, the addition of the CFTR inhibitor, CFTRinh-172 (5 μM),[40] profoundly inhibits cAMP-stimulated Cl^- permeability in Az-treated cells (Figure 7A,

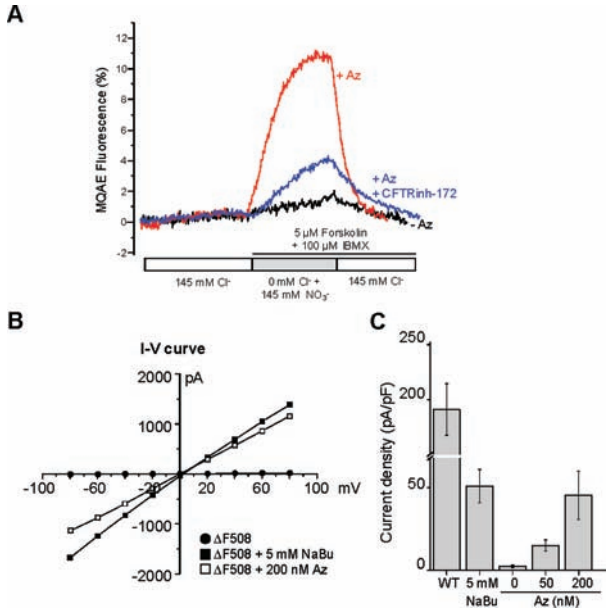

Figure 7. Az restores the Cl^- channel activity of ΔF508-CFTR. (A) Cyclic AMP-dependent chloride channel activities were examined by measuring intracellular chloride concentration changes with MQAE. (B) The current−voltage ($I-V$) relationships. Whole cell current was measured by using a patch-clamp technique in ΔF508-CFTR HEK cells that were untreated or treated with 5 mM NaBu or 200 nM Az. (C) The dose-dependent Cl^- channel activity of ΔF508-CFTR. Peak currents were normalized as currents densities (pA/pF).

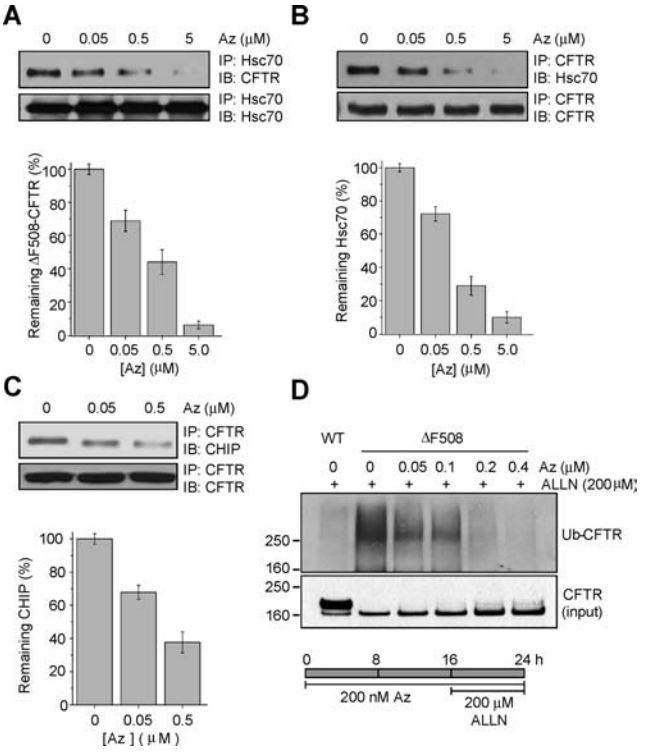

Figure 8. Az inhibits the interaction between ΔF508-CFTR and Hsc70 and CHIP to suppress ubiquitination of the mutant protein. Az treatment of ΔF508-CFTR HEK cells decreases the amount of (A) mutant CFTR coprecipitated with Hsc70, (B) Hsc70 coprecipitated with CFTR, and (C) CHIP coprecipitated with CFTR. (A−C) Lysates of ΔF508-CFTR HEK cells were exposed to various concentrations of Az for 1 h at 25 °C (mean ± SD). (D) Suppression of ubiquitination of mutant CFTR by Az. CFTR and ΔF508-CFTR HEK cells were treated with various concentrations of Az for 24 h at 37 °C. Proteasomal degradation of ubiquitinated CFTRs was blocked by 200 μM ALLN.

blue line). These findings show that functional expression of CFTR chloride channels occurs in the Az-treated cystic fibrosis cells.

The cAMP-activated ΔF508-CFTR chloride channel activity was examined also by measuring whole cell Cl^- channel currents in cells. For this purpose, patch-clamp analyses were performed on untreated and Az-treated cells. Wt-CFTR HEK cells show CFTR chloride currents in response to cAMP stimulation with forskolin and IBMX with an average current density of 191.2 ± 23.3 pA/pF (Figure 7B and C). However, no significant Cl^- channel activity activated by cAMP cocktails was observed in untreated ΔF508-CFTR HEK cells. Importantly, when ΔF508-CFTR HEK cells were treated with Az for 24 h at 37 °C, cAMP-stimulated Cl^- conductance was induced, and the chloride channel activity was inhibited by treatment with 5 μM CFTRinh-172 (Figure 7B and C, Figure S8). The activated current induced by Az was found to exhibit a linear $I-V$ relationship characteristic of CFTR. Treatment of ΔF508-CFTR HEK cells with 200 nM Az for 24 h resulted in a cAMP-stimulated Cl^- channel activity (the average current density of 40 ± 7.8 pA/pF) up to 20% of wt-CFTR cells. The effect of Az on a Cl^- channel activity was found to be concentration-dependent, with higher concentrations of Az giving rise to greater current densities and higher numbers of positively responding cells. The results obtained from MQAE and patch clamp studies support that membrane ΔF508-CFTR rescued by Az has a chloride channel function. It has been suggested that restoration of the overall level of the CFTR chloride channel activity in cells to 20−30% would be sufficient to reverse the effects of cystic fibrosis.[3] Therefore, Az has the potential of being used as a therapeutic agent to correct defects associated with the expression of mutant CFTR.

Az Disrupts Association of ΔF508-CFTR with Hsc70 and CHIP To Suppress Its Ubiquitination. To explore whether the rescue of the ΔF508-CFTR trafficking defect is a result of changes in levels of Hsc70 and other related proteins, we measured the induction of Hsc70, Hsp70, Hsp90, Aha1 (Hsp90 cochaperone), and CHIP in response to Az. The results of RT-PCR and Western blot analyses show that the expression levels of those proteins in cells are influenced very little by treatment with Az (Figures S9 and S10).

It has been shown that CHIP, an E3 ubiquitin ligase, interacts with Hsc70, which promotes ubiquitination of misfolded ΔF508-CFTR, and that the ubiquitinated mutant undergoes proteasomal degradation.[17] Accordingly, we have evaluated whether Az blocks association of ΔF508-CFTR with Hsc70 and CHIP by inhibiting the Hsc70 activity. For this purpose, the levels of coimmunoprecipitated complexes between ΔF508-CFTR and endogenous forms of Hsc70 were examined. Lysates of ΔF508-CFTR HEK cells were treated with various concentrations of Az for 1 h. Hsc70 in cell lysates was immunoisolated using anti-Hsc70 antibody, and the precipitates were probed with anti-CFTR antibody. Conversely, mutant CFTR in cell lysates was captured with anti-CFTR antibody, and the precipitates were immunoblotted with anti-Hsc70 antibody. It has been found that the amount of mutant CFTR associated with Hsc70 gradually decreases with increasing concentrations of Az (Figure 8A and B).

CHIP is associated with ΔF508-CFTR via Hsc70 to promote its ubiquitination prior to proteasomal degradation. The effect of Az on association of mutant CFTR with CHIP was examined. Mutant CFTR in HEK cell lysates treated with Az was immunoisolated with anti-CFTR antibody, and the precipitates were probed with anti-CHIP antibody. In the presence of increasing concentrations of Az, the amount of CHIP associated with CFTR gradually decreases (Figure 8C).

Because Az blocks interaction of mutant CFTR with endogenous Hsc70 and CHIP, it should suppress ubiquitination of mutant CFTR. To assess this predicted effect of Az on ubiquitination of ΔF508-CFTR, ubiquitination levels of mutant CFTR were determined. To block the degradation of ubiquitinated CFTR by the proteasome, ΔF508-CFTR HEK cells were treated with the potent proteasome inhibitor, *N*-acetyl-L-leucyl-L-leucyl-L-norleucinal (ALLN), for 8 h. Polyubiquitinated ΔF508-CFTR migrates on SDS-PAGE as a high molecular weight smear. With increasing concentrations of Az, the amount of polyubiquitinated mutant CFTR was observed to decrease in a dose-dependent manner (Figure 8D). Collectively, the data suggest that Az inhibits ΔF508-CFTR ubiquitination maybe by blocking association of the mutant with Hsc70 and CHIP.

CONCLUSIONS

Because of the difficulty in curing cystic fibrosis, which is caused by the premature degradation of misfolded ΔF508-CFTR, a large effort is underway to find small molecule correctors that restore defective cellular processing of mutant CFTR. However, the discovery of efficacious correctors is a substantial challenge due to complicated processes of CFTR maturation and translocation in which many proteins participate. It has been suggested that inhibition of Hsc70 activity can rescue defective cellular processing of mutant CFTR. Thus, inhibitors for Hsc70 are considered as potentially potent correctors that would promote membrane trafficking of mutant CFTR in the treatment of cystic fibrosis. Our results show that Az blocks the ATPase activity of Hsc70 by binding to its ATPase domain, presumably its ATP-binding pocket, and treatment of ΔF508-CFTR cells with nanomolar concentrations of Az induces the restoration of cAMP-stimulated CFTR chloride channel activity by rescuing defective membrane trafficking of the mutant CFTR. In addition, the present study suggests that Az-induced translocation of the mutant protein to the plasma membrane may be caused by disrupting the association of ΔF508-CFTR with Hsc70 and CHIP and, thus, suppression of polyubiquitination of the mutant CFTR. However, it is not ruled out that Az may affect other CFTR processing events because this molecule is also an inhibitor for Hsp70 and CFTR maturation and translocation processes are complex. Because ΔF508-CFTR translocated on the plasma membrane retains some chloride channel activity, the capability of Az to move at least some of mutant CFTR to the cell surface may have therapeutic benefit. Importantly, a combination therapy employing CFTR potentiators that lead to an increase in the functional activity of surface-expressed CFTR could represent a promising strategy for the clinical application of Hsc70 inhibitors for cystic fibrosis.

ASSOCIATED CONTENT

Supporting Information. Purification of full-length and truncated Hsc70, cell experimental procedures, and NMR spectra of Cy3-Az and **1**. This material is available free of charge via the Internet at http://pubs.acs.org.

AUTHOR INFORMATION

Corresponding Author
injae@yonsei.ac.kr; mlee@yumc.yonsei.ac.kr

ACKNOWLEDGMENT

We thank J. Pai (Yonsei University) for preparing Az-conjugated probe. This work was supported by grants from the National Creative Research Initiative, WCU (R32-2008-000-10217-0), and 2010-0001670 from the National Research Foundation of Korea (NRF).

REFERENCES

(1) Rommens, J. M.; Iannuzzi, M. C.; Kerem, B.; Drumm, M. L.; Melmer, G.; Dean, M.; Rozmahel, R.; Cole, J. L.; Kennedy, D.; Hidaka, N.; Zsiga, M.; Buchwald, M.; Riordan, J. R.; Tsui, L.-C.; Collins, F. S. *Science* **1989**, *245*, 1059–1065.
(2) Park, H. W.; Nam, J. H.; Kim, J. Y.; Namkung, W.; Yoon, J. S.; Lee, J. S.; Kim, K. S.; Venglovecz, V.; Gray, M. A.; Kim, K. H.; Lee, M. G. *Gastroenterology* **2010**, *139*, 620–631.
(3) Amaral, M. D. *Pediatr. Pulm.* **2005**, *39*, 479–491.
(4) Denning, G. M.; Anderson, M. P.; Amara, J. F.; Marshall, J.; Smith, A. E.; Welsh, M. J. *Nature* **1992**, *358*, 761–483.
(5) Ward, C. L.; Omura, S.; Kopito, R. R. *Cell* **1995**, *83*, 121–127.
(6) Ward, C. L.; Kopito, R. R. *J. Biol. Chem.* **1994**, *269*, 25710–25718.
(7) Sheppard, D. N.; Welsh, M. J. *Physiol. Rev.* **1999**, *79*, S23–S45.
(8) Gadsby, D. C.; Vergani, P.; Csanady, L. *Nature* **2006**, *440*, 477–483.
(9) Zielenski, J.; Tsui, L. C. *Annu. Rev. Genet.* **1995**, *29*, 777–807.
(10) Kerem, B.; Rommens, J. M.; Buchanan, J. A.; Markiewicz, D.; Cox, T. K.; Chakravarti, A.; Buchwald, M.; Tsui, L. C. *Science* **1989**, *245*, 1073–1080.
(11) Kopito, R. R. *Physiol. Rev.* **1999**, *79*, S167–S173.
(12) Gabriel, S. E.; Clarke, L. L.; Boucher, R. C.; Stutts, M. J. *Nature* **1993**, *363*, 263–268.
(13) Mayer, M. P.; Bukau, B. *Cell. Mol. Life Sci.* **2005**, *62*, 670–684.
(14) Hartl, F. U.; Hayer-Hartl, M. *Science* **2002**, *295*, 1852–1858.
(15) Gierasch, L. M.; Swain, J. F.; Dinler, G.; Sivendran, R.; Montgomery, D. L.; Stotz, M. *Mol. Cell* **2007**, *26*, 27–39.
(16) Scott-Ward, T. S.; Amaral, M. D. *FEBS J.* **2009**, *276*, 7097–7109.
(17) Meacham, G. C.; Patterson, C.; Zhang, W. Y.; Younger, J. M.; Cyr, D. M. *Nat. Cell Biol.* **2001**, *3*, 100–105.
(18) Younger, J. M.; Ren, H. Y.; Chen, L. L.; Fan, C. Y.; Fields, A.; Patterson, C.; Cyr, D. M. *J. Cell Biol.* **2004**, *167*, 1075–1085.
(19) Dalemans, W.; Barbry, P.; Champigny, G.; Jallat, S.; Dott, K.; Dreyer, D.; Crystal, R. G.; Pavirani, A.; Lecocq, J. P.; Lazdunski, M. *Nature* **1991**, *354*, 526–528.
(20) Sharma, M.; Benharouga, M.; Hu, W.; Lukacs, G. L. *J. Biol. Chem.* **2001**, *276*, 8942–8950.
(21) Riordan, J. R. *Annu. Rev. Biochem.* **2008**, *77*, 701–726.
(22) Amaral, M.; Kunzelmann, K. *Trends Pharmacol. Sci.* **2007**, *28*, 334–341.
(23) Verkman, A. S.; Galietta, L. J. V. *Nat. Rev. Drug Discovery* **2009**, *8*, 153–171.
(24) Pedemonte, N.; Lukacs, G. L.; Du, K.; Caci, E.; Zegarra-Moran, O.; Galietta, L. J. V.; Verkman, A. S. *J. Clin. Invest.* **2005**, *115*, 2564–2571.
(25) Rubenstein, R. C.; Zeitlin, P. L. *Am. J. Physiol. Cell Physiol.* **2000**, *278*, C259–C267.
(26) Loffing, J.; Moyer, B. D.; Reynolds, D.; Stanton, B. A. *Am. J. Physiol.-Lung C* **1999**, *277*, L700–L708.
(27) Jiang, C.; Fang, S. L.; Xiao, Y. F.; O'Connor, S. P.; Nadler, S. G.; Lee, D. W.; Jefferson, D. M.; Kaplan, J. M.; Smith, A. E.; Cheng, S. H. *Am. J. Physiol.* **1998**, *275*, C171–C178.

(28) Park, H. J.; Mylvaganum, M.; McPherson, A.; Fewell, S. W.; Brodsky, J. L.; Lingwood, C. A. *Chem. Biol.* **2009**, *16*, 461–470.
(29) Williams, D. R.; Ko, S.-K.; Park, S.; Lee, M.-R.; Shin, I. *Angew. Chem., Int. Ed.* **2008**, *47*, 7466–7469.
(30) Park, S.; Lee, M.-R.; Shin, I. *Nat. Protoc.* **2007**, *2*, 2747–2758.
(31) Williams, D. R.; Lee, M. R.; Song, Y. A.; Ko, S. K.; Kim, G. H.; Shin, I. *J. Am. Chem. Soc.* **2007**, *129*, 9258–9259.
(32) Williams, D. R.; Kim, G. H.; Lee, M. R.; Shin, I. *Nat. Protoc.* **2008**, *3*, 835–839.
(33) Chang, L.; Bertelsen, E. B.; Wisen, S.; Larsen, E. M.; Zuiderweg, E. R. P.; Gestwicki, J. E. *Anal. Biochem.* **2008**, *372*, 167–176.
(34) Tsukiji, S.; Miyagawa, M.; Takaoka, Y.; Tamura, T.; Hamachi, I. *Nat. Chem. Biol.* **2009**, *5*, 341–343.
(35) Williamson, D. S.; Borgognoni, J.; Clay, A.; Daniels, Z.; Dokurno, P.; Drysdale, M. J.; Foloppe, N.; Francis, G. L.; Graham, C. J.; Howes, R.; Macias, A. T.; Murray, J. B.; Parsons, R.; Shaw, T.; Surgenor, A. E.; Terry, L.; Wang, Y.; Wood, M.; Massey, A. J. *J. Med. Chem.* **2009**, *52*, 1510–1513.
(36) Muller, K.; Faeh, C.; Diederich, F. *Science* **2007**, *317*, 1881–1886.
(37) Cheng, S. H.; Fang, S. L.; Zabner, J.; Marshall, J.; Piraino, S.; Schiavi, S. C.; Jefferson, D. M.; Welsh, M. J.; Smith, A. E. *Am. J. Physiol.* **1995**, *268*, L615–L624.
(38) Okiyoneda, T.; Barriere, H.; Bagdany, M.; Rabeh, W. M.; Du, K.; Hohfeld, J.; Young, J. C.; Lukacs, G. L. *Science* **2010**, *329*, 805–810.
(39) Choi, J. Y.; Muallem, D.; Kiselyov, K.; Lee, M. G.; Thomas, P. J.; Muallem, S. *Nature* **2001**, *410*, 94–97.
(40) Ma, T. H.; Thiagarajah, J. R.; Yang, H.; Sonawane, N. D.; Folli, C.; Galietta, L. J. V.; Verkman, A. S. *J. Clin. Invest.* **2002**, *110*, 1651–1658.